e-Prime - Advances in Electrical Engineering, Electronics and Energy 9 (2024) 100755

Contents lists available at ScienceDirect

e-Prime - Advances in Electrical Engineering, Electronics and Energy

journal homepage: www.elsevier.com/locate/prime

Optimal utilization of frequency ancillary services in modern power systems

Kaleem Ullah [a], Zahid Ullah [b], Abdul Basit [c], Giambattista Gruosso [*,b]

[a] US-Pakistan Center for Advanced Studies in Energy, University of Engineering and Technology Peshawar, Peshawar, 25000, Pakistan
[b] Dipartimento di Elettronica, Informazione e Bioingegneria, Politecnico di Milano, Piazza Leonardo Da Vinci, 32, Milan, 20133, Italy
[c] Manager R&D, National Power Control Center, National Transmission and Dispatch Company, Islamabad, 44000, Pakistan

ARTICLE INFO

Keywords:
Wind Energy Systems
Coal-based Energy Systems
Power Dispatch Strategies
Frequency Regulation
and Automatic Generation Control

ABSTRACT

The widespread global adoption of wind energy sources has established a significant presence in the existing power grid. However, the massive integration of intermittent wind energy poses forecasting errors, prompting the need for supplementary reserves from conventional energy sources with increased operational expenses and carbon emissions. Hence, to facilitate the seamless operation of large-scale wind-integrated power grids, it is imperative to harness the potential of renewable energy sources and leverage flexible loads to deliver power-balancing services. In this research, dynamic real-time power dispatch strategies have been developed for the Automatic Generation Control (AGC) system to integrate the reserve capacities of conventional generation units and wind power plants and utilize the demand response capabilities of flexible loads for power balancing services. A comprehensive power system grid model was developed in DigSilent PowerFactory software, consisting of coal-based energy systems, wind energy systems, gas turbines, and cold storage units as flexible loads. The study is divided into different case studies to assess the impact of each scenario on system operation in mitigating the forecasting errors of wind power plants. Further, a comparative analysis was performed to illustrate the effectiveness of each case study. The analysis showed that Case Study III, where reserves are provided by coal energy systems and cold storage units, yielded the highest reduction in Positive Regulation (PR) and Negative Regulation (NR) errors, at 89.0% and 94.15%, respectively. Conversely, Case Study IV demonstrated the least reduction in errors, with 67.82% in PR and 78.41% in NR. However, it indicates that reserves can be supplied from wind energy systems and flexible loads without the support of conventional power plants.

1. Introduction

1.1. Background

The worldwide massive integration of wind energy resources into power systems represents a pivotal milestone in the shift toward sustainable energy solutions [1,2]. However, the massive integration of wind energy poses forecasting errors due to inherent intermittency associated with renewable energy resources. The intermittency of wind energy occurs due to variable wind speed. Therefore, there is an emergent need to deal with forecasting errors and ensure the reliable and efficient integration of clean and renewable energy resources [3,4]. The accurate predictions of wind speed assist in mitigating forecasting errors and provide a reliable power supply. Therefore, power system operators employ various scheduling methodologies to balance the demand and supply. These methodologies assist in mitigating the inaccuracies of power imbalances due to forecasting errors using additional energy reserves from traditional generating units. However, using additional reserves from conventional power plants incurs higher CO_2 emissions and operational costs. In this regard, the large-scale integration of wind energy into a conventional power grid is analyzed to assess the requirement of additional reserves from traditional generating units [5]. Further, it was revealed that intermittent and stochastic wind speed significantly increased the need for reserve utilization from conventional energy resources to keep the power balance. However, the massive integration of wind energy ensured an active power balance and maximized wind energy utilization. Therefore, there is a need to integrate reserves from wind power plants effectively. To address this, developing a refined model of wind power plants that can operate at lower capacities and maintain reserves when required is necessary. Additionally, flexible loads, such as cold energy units, benefit power systems substantially due to their dynamic load characteristics. These

* Corresponding author.

https://doi.org/10.1016/j.prime.2024.100755
Received 10 April 2024; Received in revised form 5 August 2024; Accepted 28 August 2024
Available online 3 September 2024

units' energy storage capabilities and flexible consumption patterns present a viable solution for frequency regulation in power grids. This study proposes an innovative solution for the AGC system, integrating reserve power from wind power plants and utilizing the demand response capabilities of cold storage units. This approach aims to maintain the power balance between load and generation in large-scale wind energy-integrated power grids, ensuring a more stable and reliable energy supply.

1.2. Literature review

Extensive research studies explored the power-balancing capabilities of wind power plants [6–9]. For instance, the authors in [10] examined the operational efficacy of an 800kW IEC Type 4 wind turbine in Saskatchewan, Canada, concerning its provision of secondary frequency response through AGC in modern power systems. Using PJM methods, performance scores were computed, revealing an impressive 59% and 65% surplus and deficit about rated wind speeds, respectively. Despite achieving the minimum performance score, it is demonstrated that deploying wind power in the regulation market yields superior profitability compared to other traditional technologies. The authors in [11] presented a cost-effective solution to alleviate line congestion in a power grid with high wind integration. A dispatch approach for the LFC model is developed to manage power flow during the dispatch process. The power flow is controlled in a manner that considers the impact on the power flow threshold in the associated lines. In [12], an attempt has been made to address the forecasting error challenge within wind-dominant power grids. This is achieved by integrating reserve power sourced from Electric Vehicles (EVs) and coal-based power grids. The authors in [13] analyzed the factors associated with the effectiveness of wind turbine response that can be achieved through the availability of an abundant wind supply, coupled with the turbine and prompt response to the power command signal originating from the AGC unit. Type IV wind turbines are more efficient in harnessing wind power from the grid owing to their distinct systems at the machine and grid interfaces. This technology is trialed on the Danish power network, employing various power dispatch techniques to enhance the optimal utilization of wind power and alleviate the strain on their traditional power grid [14,15]. Energy storage systems are viable for tackling forecasting error issues of wind energy sources [16]. However, the operational costs experience a noticeable increase that poses a challenge to its practicality in providing active power regulation services to the grid.

The authors in [17] extensively reviewed the AGC concept in RES-based interconnected power systems, including the HVDC connections. Further, the review covers AGC difficulties on FACTS, energy storage, high renewable integration, negative control schemes of EVs, and fractional-order controllers. In [18], the authors presented the design, implementation, and assessment of interlinked hydropower systems in a de-regulated environment with energy storage equipment. The optimal performance of the energy storage devices was tested for various transactions and under different conditions. Calculations prove that the OC fulfills AGC criteria, with the RFB demonstrating a more effective operation. A new structure for the cascaded control system based on FOID and FOPIDN controllers optimized via the Archimedes optimization algorithm (AOA) is provided [19]. Conducted on a two-area microgrid with different power feeders, the AOA tuned CFOID-FOPIDN controller exhibits much less settling time and much higher performance than other controllers in all testing conditions. The authors in [20] developed a FOFPID controller for LFC in a multi-micro grid system incorporating renewable and hybrid energy systems. The parameters of the FOFPID controller are fine-tuned with the modified Harris Hawks Optimizer (mHHO), which offers even better optimization than other optimization techniques and improves the frequency regulation. In [21], the authors outlined the capability and objective of ASEAN in terms of the usage of renewable energy and their ultimate goal of reaching 23% of renewable energy use, in addition to reducing greenhouse gas emissions. The authors in [22] systematically and sustainably selected and modeled a solar/wind/battery/diesel microgrid for the Pabna University of Science and Technology with reliable power system performance and cost/emission minimization considerations. The account also stresses the versatility of the microgrid in achieving a 23. 31 kW peak load and claims to feed power back into the electric grid during power outages. In [23], the authors increased the transmission line's load capability by using a novel voltage stability index, the rapid voltage stability index, and the grey wolf algorithm on the IEEE 30-bus system, thus minimizing congestion and reducing fuel costs. Maximally applied in MATLAB, the proposed methodology handles voltage instability while minimizing generation costing, polluting emissions, and line energy losses. The authors in [24] utilized a new algorithm called horse herd optimization for maximum power point tracking (MPPT) and the Raspberry Pi Pico controller. With the change of the generated power in the cascaded buck-boost converter, the system's efficiency can be optimized to work for solar trees under dynamic shading conditions and increase solar energy utilization efficiently and sustainably. In [25], the authors developed the Nataf-Kernel Density-Spline-based point estimate method (PEM) for probabilistic load flow (PLF) studies to improve the accuracy of the WGOP by employing the technique, which performs better than conventional PEM and Monte Carlo simulations. The authors in [26] assessed the optimization techniques of the Isolated/Hybrid microgrid system on the Perhentian island. HOMER software found out that HOMER has the lowest convergence time and NPC. Advanced PID and Fuzzy Logic Controllers mean regulation of voltage and varying frequency. A selective one-stage high voltage DC-DC converter improves the output solar photovoltaic power quality with low reverse recovery currents and voltage stress and improved output voltage. An enhanced Real-Time PI controller and a Real-Time Neural Network controller have been proposed, and their effectiveness is supported by MATLAB/Simulink simulations [27].

In [28], the authors demonstrated that flexible loads provide ancillary services, like secondary and tertiary regulation, curbing the operator's need to predict and oversee large-scale wind-integrated power systems. Leveraging flexible loads can cut system costs by reducing reliance on conventional power generation. Flexible loads can adapt their energy utilization temporarily to provide supplementary services while maintaining their primary function [29]. The study also provided approximations for flexible load units in Denmark in 2020, encompassing 76,500 EVs and 250 MW of cold storage capability, summing up to a total capacity of 600 MW. These dynamic load resources effectively react to peak demand periods, redistributing the load to enhance the efficiency of power distribution within the existing grid infrastructure. As a result, this diminishes the necessity for supplementary backup reserves, guaranteeing system stability without acquiring additional costs [30,31]. The authors in [32] presented an innovative integrated strategy that integrated the building heating loads into a comprehensive community energy system. The primary goal was to improve scheduling power production and usage efficiency. Additionally, buildings account for approximately 40% of worldwide energy consumption, with heating and cooling constituting 50%. Conversely, EVs can serve as flexible loads due to their inherent characteristics that make them adaptable. In [33–36] the authors examined the role of EVs as energy storage systems in AGC services using V2G technology. This, in turn, facilitated a two-way power flow between the power systems and EVs.

1.3. Research gap

Despite the extensive research on AGC, numerous articles have explored various issues, including constraints, small signal stability, AGC in non-linear models, and the calibration and implementation of AGC in single and multi-area power system configurations. Additionally, AGC systems incorporating energy storage devices, HVDC transmission, FACTS, and the integration of RESs have been addressed. However,

there remains a notable gap in research on AGC systems that combine reserves from RESs with conventional energy systems, which has the potential to reduce operational costs and CO2 emissions. Furthermore, applying demand response for flexible loads in AGC systems has seen limited progress.

1.4. Contributions of the paper

Considering the aforementioned research works, this study utilizes the reserve capacity of wind energy systems and the demand response application of cold storage units to maintain grid stability during power balancing operations. The primary objective was to develop and compare real-time dynamic dispatch strategies for the AGC system, covering different scenarios to efficiently address power imbalances due to wind forecasting errors in power systems. Four case studies were analyzed and compared quantitatively and using graphical illustrations. The first case study integrated the operational reserves solely from coal-based energy systems (CESs) and achieved a reduction of 84.4% in positive regulation error (PR) and 82.79% in negative regulation error (NR). The second case study integrated the wind power reserves along with the CES to perform the power balancing operation, resulting in slightly better reductions of 86.24% in PR error and 82.79% in NR error. Case study 3 was the most effective, with reductions of 89% in PR error and 94.15% in NR error by utilizing the reserve capacity of CESs with the demand response of cold storage units. Case study 4 was the least effective, with reductions of 67.82% in PR error and 78.41% in NR error. However, in this case study, reserves were utilized solely from the cold-based storage units and the wind energy system, thereby eliminating dependency on conventional power plants. A comprehensive model is developed using DigSILENT Power Factory software to evaluate the proposed dispatch strategies. This proposed model incorporated various power generation units, such as CESs, Wind Power Energy Systems (WPESs), Gas Turbine Power Plants (GTPPs), and Cold Storage Units (CSUs). Governors were designed for the generating units to provide a primary response at the distributed level. However, a centralized AGC model is developed for secondary regulation. The pertinent contributions are as follows.

- A comprehensive power grid network is developed, incorporating detailed models of CESs, GTPPs, WPESs, and CSUs. The generating units are equipped with governors to provide the required primary response before the activation of AGC reserves.
- A centralized AGC system is modeled for the power grid to ensure essential frequency support during grid balancing operations. The AGC model is incorporated with the following dispatch-designed strategies: (a) AGC Dispatch with CESs Only, (b) AGC Dispatch with CESs and WPESs, (c) AGC Dispatch with CESs and CSUs, and (d) AGC Dispatch with WPESs and CSUs.
- A comprehensive comparative analysis is performed utilizing graphical and quantitative techniques to assess each dispatch strategy's effectiveness in enhancing the designed AGC system's secure and cost-efficient operation.

1.5. Organization of paper

This remainder of the paper is structured as follows: Section 2 presents a comprehensive modeling of generation units (CESs, GTPPs, WPESs, and CSUs) and provides detailed AGC unit modeling, integrating the generating units and CSUs. Section 3 explores multiple case studies demonstrating the development and implementation of the dispatch above strategies in the AGC model, providing practical insights and analysis. Section 4 conducts a comparative quantitative analysis, carefully comparing and analyzing the outcomes of the four case studies. Section 5 provides a detailed summary of the proposed work.

2. Modelling of the proposed power GRID

This study considered a comprehensive power grid model, incorporating the power-generating models of CESs, GTPPs, and WPESs. A CSU model is developed for the AGC system and integrated into the grid. Further, the proposed power grid is interconnected with another grid, capable of supporting the grid frequency at a rate of 6060 MW/Hz. Fig. 1 shows the detailed connectivity of the proposed system, where the dotted line represents information, and the solid line represents the power network flow. Moreover, the connectivity of different generating units with the AGC model is illustrated in Fig. 1. The integrated AGC model continuously senses the supply-demand error, providing feedback on the required power from the generating units based on the designed dispatch strategies. In this study, operating reserves for the secondary control (AGC) are installed on the CESs, WPESs, and CSUs. The gas turbine is integrated into the system to provide power and primary response only. The detailed modeling of the generating units is provided in the following subsections.

2.1. Modelling of coal-based energy system

This research paper employs the aggregated model of the CES to assess its capabilities in power balancing services [12]. Fig. 2 represents the complex CES model that generates frequency regulation responses. The P_{mech} harnessed from the section of the steam turbine is contingent upon two input factors: the regulation control valve (cv) acquired from the governor block and steam pressure (P_t) is derived from the boiler control section. The response time from the boiler is the key factor on which the entire model of the plant is based, as it plays a pertinent role in the overall reaction of the unit. The response of the boiler requires approximately 5-6 minutes, which strongly influences the general behavior of the turbine. When the reference point of the load L_R deviates in response to any variations, the boiler control unit computes changes and stabilizes the main P_t with precision.

The model includes generator reference current and temperature constraints, ensuring the change rate does not exceed 29 MW/m. The time delays associated with the steam storage system of the unit (b_1, b_2 and P_t) mainly impact the unit's response to any variation in the system frequency. A cross-compound double reheat steam turbine is utilized in the study that generates mechanical power based on the response of the boiler model (P_t) and the output of the governor (cv). Further, the four-time constants, specifically T_1, T_2, T_3, and T_4 govern the turbine's response and characterize the charging process of components. The precise quantification of each section of turbine contribution to the overall mechanical output is accomplished by utilizing coefficients K_1 through K_8. Specifically, K_1, and K_2 pertain to the highly critical, very high-pressure section, while K_3, K_4, K_5, K_6 represent the elevated and intermediate pressure sections correspondingly. Lastly, K_7,and K_8 correspond to the lower-pressure section. The speed governor effectively harnesses changes in droop settings and generator speed as essential input parameters for delivering the primary frequency response.

2.2. Modelling of gas turbine power plant

The Proposed model of the GTPPs is shown in Fig. 3 [12]. However, in this study, it is simplified to analyze its performance in grid regulation services. When the deviations in the power grid exceed the pre-established dead band thresholds, the system frequency changes. The resulting frequency fluctuations are transformed into a power demand signal (ΔP_c) by implementing the droop mechanism. This power demand signal assumes a key role as an input to the GTPP, which encompasses the Power limitation section (PLS), distribution section (PBS), and gas turbine dynamics section (GTDS). Considering the limitations of combustion technology, the PLS element enforces physical constraints on the response of the turbine output. At the same time, the PLS module accepts both the ΔP_c and reference power signals as inputs,

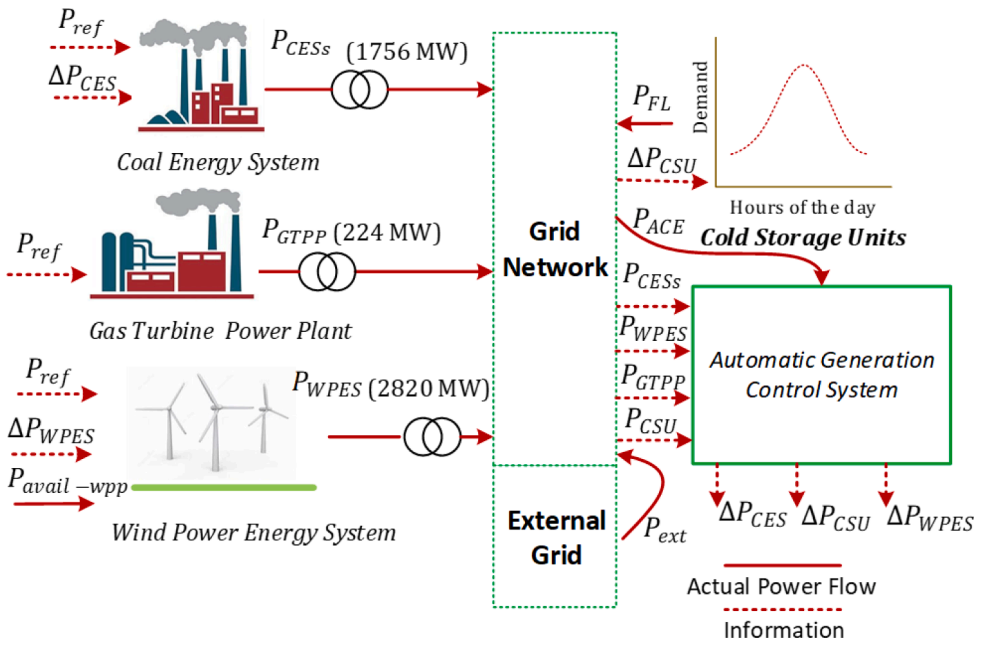

Fig. 1. Proposed Power Grid with AGC model.

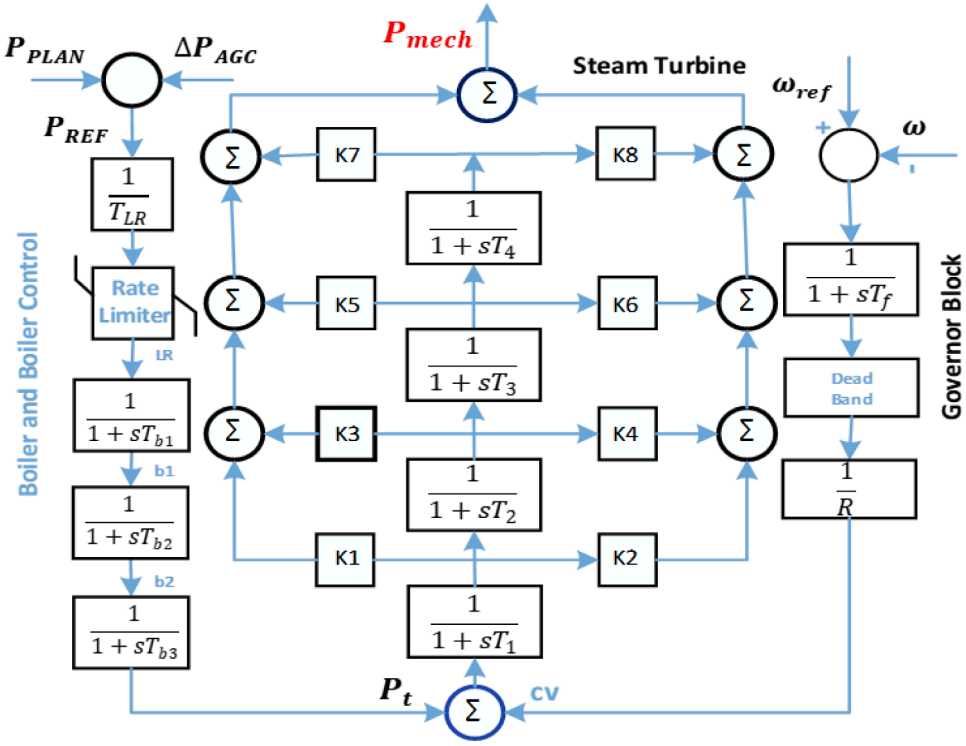

Fig. 2. Coal Based Energy System Model.

generating a command signal (CLC) for the PBS section. This module encompasses two sequential combustion chambers. The initial chamber receives pressurized air, undergoes thermal elevation, and amalgamates it with 50 percent of the total fuel constituent. The resulting mixture is then expelled via the high-pressure turbine and channeled into the SEV chamber, where 50 percent of the remaining fuel is united with supplemental air. Following the heating process, the mixture is subsequently directed through a low-pressure turbine renowned for its exceptional operational versatility, minimal emission levels, and remarkable efficiency. The dynamics of the environmental and sequential environmental combustors are modeled using a first-order lag function. In contrast, a second-order function denotes the variable inlet guide vanes dynamics. The GTPP demonstrates a robust overall response time of approximately 30 to 40 seconds for any adjustments in the system frequency.

2.3. Modelling of wind power energy system

Fig. 4 illustrates a WPES to investigate wind farm dynamics in supporting power grid balancing operations [37]. However, a simplified

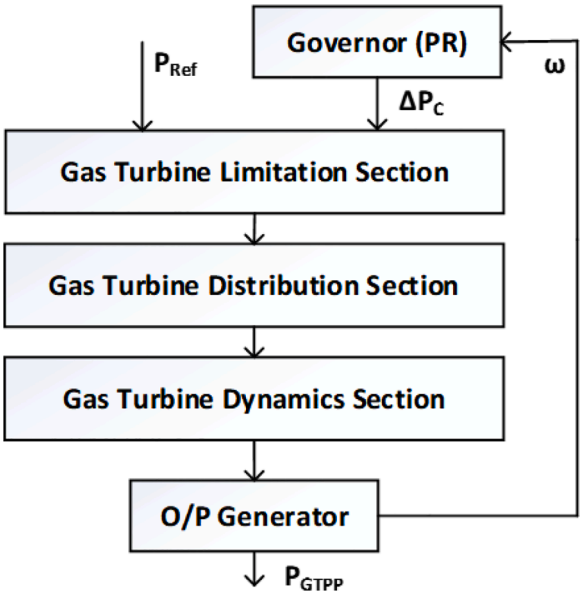

Fig. 3. Gas Turbine Power Plant System.

model analyzes its performance in active power balancing services. The proposed model is established upon the guidelines set forth by the IEC61400-27-1 committee. The model encompasses three key blocks: the wind turbine active power regulator (WTAPC), the wind power energy system active power regulator (WPESAPC), and the reference current section of the generator. Moreover, the governor, encompassing droop attributes, imparts the primary frequency response (ΔP_c) that relies on wind availability ($P_{WPESavail}$) and the system's frequency droop parameters.

The WPESAPC block achieves optimal performance by generating the turbine reference power (P_{ref_WT}). Whenever there is a modification in the reference power of the WPES (P_{ref_WPES}). The calculation of (P_{ref_WPES}) relies upon a multitude of factors, such as the reference power signal (P_{ref}) and the primary (ΔP_c) signal, the power measured at the PCC (P_{meas_PCC}). Adapting continuously to the prevailing conditions, the PI controller encapsulated in the WPESAPC unit diligently adjusts the baseline signal intended for the WTAPC unit based on the disparity signal derived from P_{ref_WPES} and P_{meas_PCC}. The available power constrains the output of the PI regulator signal $P_{WPESavail}$. Concurrently, the WTAPC block generates the active component of the generator current I_{pcmd}, computed by the PI regulator, considering the variation between the P_{meas_PCC} and P_{ref_WT}. Type IV wind turbines are used in this study. They are distinguished by their incorporation of machine-side and grid-side converters and autonomous operation. Considering wind power availability, the reference value is subject to a ramp-rate restriction to ensure controlled operation. Notably, the WPES exhibits remarkable responsiveness to alterations in system load, typically manifesting within a short timeframe ranging from 2 to 4 seconds.

2.4. Cold storage unit modelling as a flexible load

Temperature control loads, such as CSUs, possess the capacity to offer required regulatory services owing to their precise temperature regulation capabilities. The CSUs can be regarded as versatile loads with a certain level of regulatory adaptability. Grid operators can access backup reserves from CSUs through demand response mechanisms, permitting them to remotely tune the temperature settings of these loads during periods of higher electricity demand or limited supply. The ongoing reduction in power consumption from CSUs can serve as available reserves for system operators to provide frequency regulation services. This can be achieved through the AGC, wherein the power output from the CSUs can be regulated analogous to power generation units. The energy equilibrium within the domain of cold storage can is expressed as follows [32].

$$\gamma_{\tau_p}\frac{dT_{\tau_p}}{dt} = \frac{dQ_l}{dt} - \frac{dQ_e}{dt} \tag{1}$$

Here, γ denotes the complete mass of frozen commodities, while τ_p indicates the distinct heat capacity of the frozen items. Q_e and Q_l correspond to the cooling potential of the refrigerated chamber and surrounding atmosphere. Further, (2) and (3) establish the potential loads that cold storage systems can accommodate, while (4), (5), and (6) illustrate the state and control parameters [32].

$$\frac{dQ_l}{dt} = (\nu A)_{m\_c.}(T_m - Ta) \tag{2}$$

$$\frac{dQ_e}{dt} = (\nu A)_{cr\_e.}(T_r - Te) \tag{3}$$

$$T_{cr,mn} \le T_r \le T_{cr,mx} \tag{4}$$

$$0 \le T_r - T_e \le \infty \tag{5}$$

$$0 \le \frac{dQ_e}{dt} \le (\nu A)_{cr\_e.} max(T_r - T_e) \tag{6}$$

Here, (3) and (6) provide insight into the thermal conduction coefficient, denoted as νA. The ambient air temperature is denoted as T_m, and the overall temperature range inside the CSUs is represented by $T_{r,mn}$ and $T_{r,mx}$ range. Furthermore, the refrigerator's temperature is T_e at its boiling point. However, the compressor operator regulates the

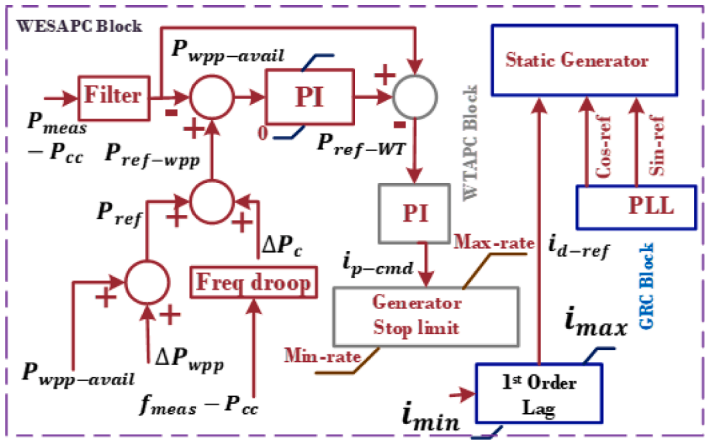

Fig. 4. Wind Power Energy System.

evaporative stage temperature, ensuring that T_e is always less than or equal to T_r. The energy balance equation addresses the dynamics and limitations of the cold storage unit, primarily influenced by the mass flow rate (m_r) and the associated changes in energy content (ω_c) [32].

$$m_r = \frac{\frac{dQ_e}{dt}}{h_{oe}(T_e) - h_{ie}(T_c)} \tag{7}$$

Equation (7) establishes the m_r while (8) calculates ω_c considering the difference between the refrigerant's enthalpy at the compressor's entrance h_{ic}, and its departure h_{oe}. It is crucial to emphasize that isentropic efficiency, denoted as η_{ic}, is presumed to persist constant within the predefined operative range. Here, $\wp_c$ and $\wp_e$ denote the refrigerant pressures at the compressor's inlet and outlet.

$$\frac{d\omega c}{dt} = \frac{m_r(h_{oe}(T_e, \wp c) - h_{ic}(T_e)}{\eta_{ic}\left(\frac{\wp_c}{\wp_e}\right)} \tag{8}$$

2.5. AGC modelling

The implementation of AGC is essential to achieve a highly efficient, reliable, and safe electricity supply within an interconnected power network. The AGC system continually monitors changes in power consumption and adjusts generator output accordingly. Tie-line power transfers and variations in frequency represent two essential factors employed in the AGC service to derive the direct equation for Area Control Error (ACE). The most significant step in AGC control is the calculation of $P_{ACE,i}$, expressed mathematically as follows:

$$P_{ACE,i} = \sum_{j \in A_n} \beta_i \Delta f + \left(P_{ij}^{Sch} - P_{ij}^{Act}\right) \tag{9}$$

Here, $P_{ACE,i}$ refers to cumulative deviation in the ith control area. The scheduled and actual power exchanges across the tie line are represented as P_{ij}^{Sch} and P_{ij}^{Act}, respectively. The tie-line error (ΔP_{tie}) refers to the disparity between these two values. β_i (frequency bias constant) is expressed as $\beta_i = D_i + 1/R_i$, where R_i and D_i represent network damping and droop, respectively. Δf refers to the difference between the overall frequency value and its deviation. During the mismatch between supply and demand, the speed governor promptly initiates the mobilization of the frequency containment reserve (FCR), while concurrently, the AGC perceptively detects the fluctuations in $P_{ACE,i}$ and triggers the Fast Reserve Response (FRR) to regulate $P_{ACE,i}$ and preserve the primary reserves for subsequent utilization. The AGC controllers diligently fine-tune the reference point ($\Delta P_{ref,i}$) of all generating units concurrently, harmoniously striving to attain the objective. The AGC model in Fig. 5 employs a PI regulator to mitigate effectively P_{ACE} using (10).

$$\Delta P_{Sec} = K.\Delta P_{ACE} + KT \int \Delta P_{ACE}\, dt \tag{10}$$

3. Case studies

This section presents different case studies to analyze the system operation when subject to forecasting errors associated with the massive integration of wind energy. Fig. 6 depicts the initial power imbalances present in the network due to forecasting errors of intermittent wind speed. These power imbalances necessitate the utilization of balancing reserves from various energy systems through the proposed AGC system for mitigating forecast errors. Table 1 lists the predefined capacities and reserves for regulating generation units and flexible loads for all case studies.

3.1. Case study 1: AGC dispatch with CES only

The preliminary case study conducts a comprehensive simulation analysis to assess the proposed AGC system efficacy exclusively within the CESs. Though CESs exhibit a commendable capacity to furnish ample reserves for regulation, their extensive reliance on conventional fuels gives rise to high operational expenses and exerts significant environmental concerns. The simulation parameters are calibrated according to the values outlined in Table 1. CESs are designated for AGC implementation in this specific scenario, adhering to the devised dispatch strategy outlined in Fig. 7. Fig. 8 (a) compares the AGC-incorporated output of the CESs with the ACE, arising due to the power imbalance.

Fig. 8 (b) illustrates the active involvement of CES in the system response at the secondary level when $P_{ACE} \neq 0$. In such instances, the AGC diligently triggers the secondary reserves of CES, effectively curbing power surpluses or deficits and minimizing the steady-state frequency deviation. However, it is imperative to recognize that the value of P_{ACE} may surpass the prescribed threshold of Ø100MW, which delineates the limit of the secondary reserve of CES. Secondary reserves extracted mainly from CESs significantly diminish power disparities within the Ø100MW scope. This is depicted in Fig. 8 (c), where a

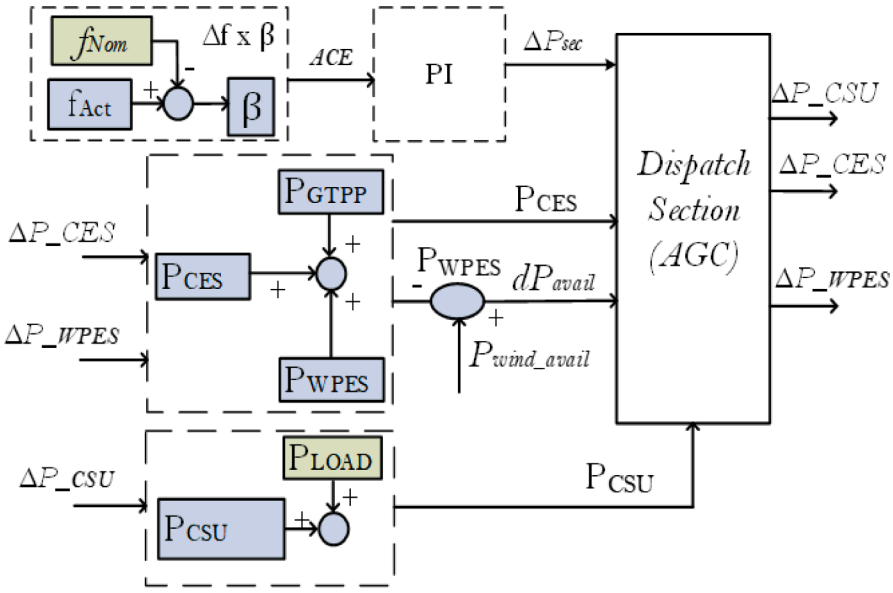

Fig. 5. Proposed AGC model.

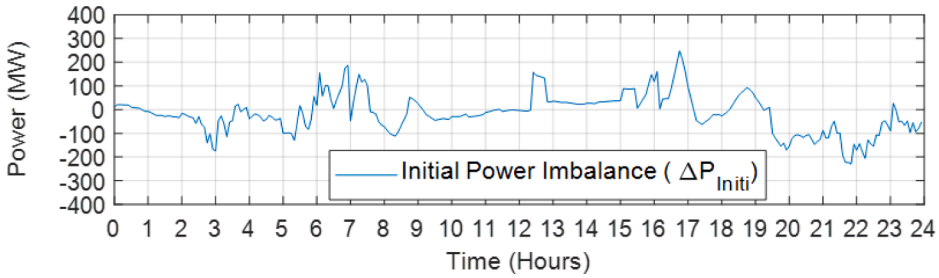

Fig. 6. Initial Power Imbalance in the system.

Table 1
Generating Units and CSUs Parameters for Case Studies.

Generating Units (MW)	GTPPs	CESs	WPESs	CSUs
Capacities (MW)	224	1756	2820	-
AGC Reserves (MW)	0	Ø100	-440	Ø75

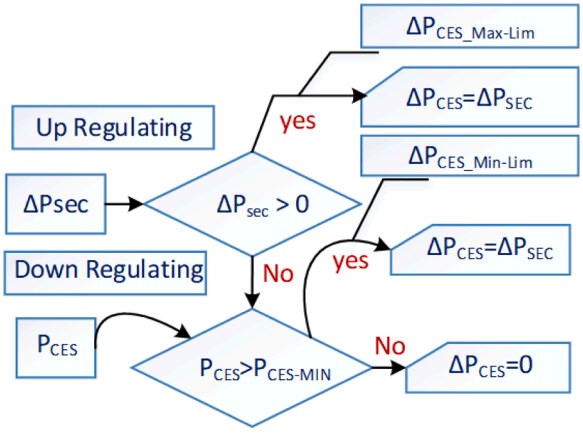

Fig. 7. CESs involvement in Secondary Dispatch Process.

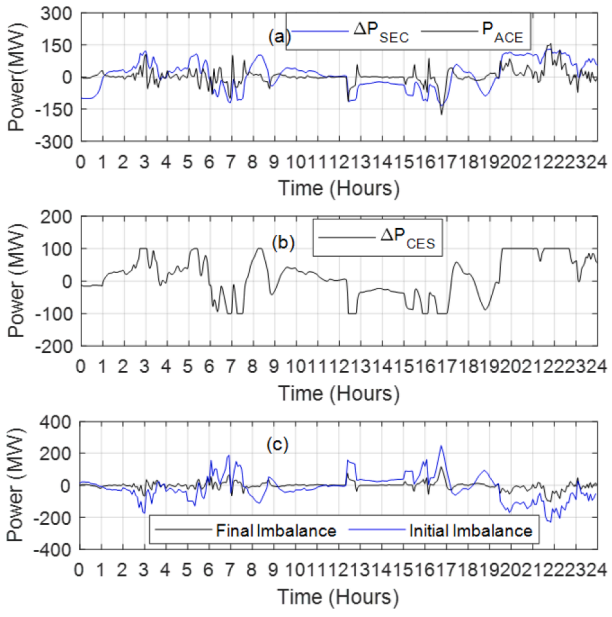

Fig. 8. (a) AGC Dispatch following area control error (b) CES dispatch (c) Comparison of power imbalances.

comparative examination of the initial and final power imbalances following the AGC response is showcased. Consequently, persistent deviations in the system's steady-state frequency occur, as clearly illustrated in Fig. 9.

3.2. Case study 2: AGC dispatch with CES and WPES

This subsection integrates reserves from the WPESs into the AGC system alongside CESs. The wind farm activates the delta production constraint function to achieve up and down regulatory power. In adherence to regulatory standard TF 3.2.5, a grid-interconnected wind turbine, functioning at a voltage surpassing 100 kV and manifesting a delta production constraint function, regulates power supply by constraining the power output derived from the continuous generation of WPESs. Consequently, a predetermined power portion is dedicated to effectively addressing regulatory demands. However, wind turbine operation under such a mode exacerbates the operational costs associated with a WPES. This investigative research uses a method to integrate WPES in the AGC model, specifically tailored to tackle power variations when generation effectively exceeds the loading power. The dispatch strategy depicted in Fig. 10 revolves around the primary objective of cost optimization. The wind energy reserves are exclusively utilized when an excess of generation $\Delta P_s < 0$ is detected, while CES reserves, amounting to Ø 100MW, are employed to tackle excess and deficient generation scenarios.

Further, the output of the WPES is curtailed solely in case of CESs operating at their minimum limit ($\Delta P_{CESs,min}$), or AGC secondary dispatch is reached at a lower limit ($\Delta P_{CES,min}$) that is set at -100 MW. In scenarios where the CES fails to actively participate in the regulation process, the dispatch of WPESs is adjusted to mitigate the remaining power P_{ACE} by decreasing energy output. However, in instances of positive regulation $\Delta P_s > 0$, the response from WPESs is not feasible as wind turbines operate at peak capacity, triggering the activation of the secondary reserves of the CESs. This action leads to a decrease in both CO2 emissions and operational costs. The P_{ACE} and ΔP_{Sec} signals representing the collective secondary dispatch are depicted in Fig. 11 (a), where the ΔP_{Sec} signal exhibits a time delay in comparison to the P_{ACE} signal due to power plant response and AGC system delay. Fig. 11 (b) shows the individual reactions of ΔP_{WPES} (WPES) and ΔP_{CES} (CES) to the ACE signal. The WPES adjusts its production solely based on the AGC command when the CES operates at its worst generation threshold, set at 20% of the online capacity. or when the ΔP_{CES} reaches a lower threshold

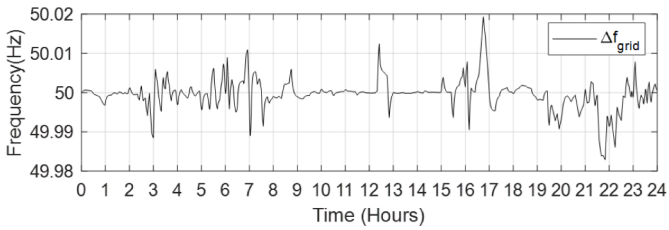

Fig. 9. Power frequency following AGC response.

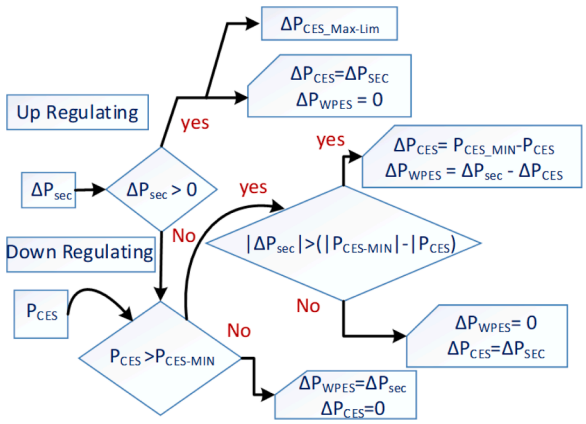

Fig. 10. Participation of CESs and WPES into Secondary Dispatch Process.

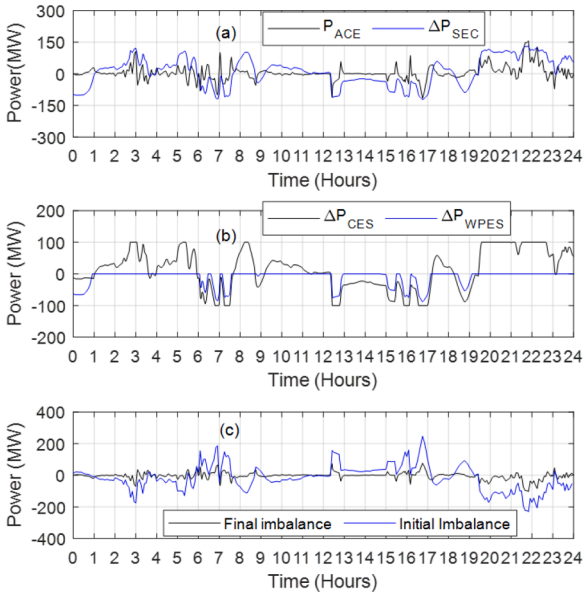

Fig. 11. (a) AGC Dispatch following area control error (b) individual dispatch of CES and WPES (c) Comparison of power imbalances.

of -100 MW. The equilibrium state frequency resulting from the AGC's response is illustrated in Fig. 12, further exemplifying the effectiveness and impact of this approach.

3.3. Case study 3: AGC dispatch with CES and CSU

The subsection above demonstrated that CSUs can offer effective frequency support to the grid when used alongside conventional energy systems. Hence, CSUs provide a compelling solution for regulating reserves that effectively mitigate power imbalances within the grid. Hence, CSUs alleviate the system operator's burden of managing a power system intricately intertwined with wind power. As depicted in

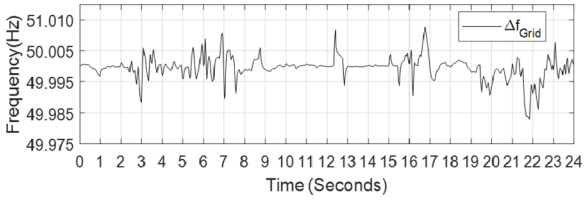

Fig. 12. Power frequency following AGC response from CES and WES.

Table 1, the CSUs can offer a substantial capacity of Ø75 MW for power regulation. Hence, any noticeable shift in the network frequency leads to the P_{ACE}. The AGC quickly addresses this situation using AGC services sourced from the CES and the CSUs. The urgent mismatches between the changing power demand and generation are mitigated by utilizing extra power reserves from the CES and the CSUs. Fig. 13 illustrates an optimized dispatch strategy developed with a consistent emphasis on cost factors. Compared to case study 2, the CSU is innovative in adjusting upward and downward power imbalances.

Fig. 14 (a) shows the cumulative secondary dispatch ΔP_{Sec} of participating generating units' secondary response, aligning with the P_{ACE} signal. Fig. 14 (b) shows the secondary dispatch originating from the generating units ΔP_{CES} and ΔP_{CSU}. The evident trend in Fig. 14 (b) suggests that CESs singularly respond once the CSU's cumulative reserve power is depleted during up-regulation. In contrast, the reverse scenario is evident during down-regulation, where the CES initiates its response before engaging the CSUs. Therefore, CES operates at a lower capacity during up- and down-regulation scenarios. Fig. 14 (c) presents a comparative examination of the real-time power balancing error preceding and after the AGC activation, where a reduction in power imbalance is depicted during periods of excessive generation and generation shortfall. Further, Fig. 15 illustrates the steady-state system frequency, providing a graphical depiction of its stability.

3.4. Case study 4: AGC dispatch with WPES and CSU

This Case study attempted to integrate operating reserves only from WPESs and CSUs, thus eradicating the need for conventional reserve power. Fig. 16 illustrates the proposed dispatch strategy activating secondary reserve based on cost optimization.

The CSUs demonstrate their versatility by adjusting positive and negative regulation processes. However, when the CSUs' regulation capacity is completely depleted, the WPESs consistently operate at maximum output, responding only during negative regulation. During the power balancing operation, the responsibility of the secondary response, as revealed in Fig. 17 (a), was solely entrusted to the WPES and CSU. In Fig. 17 (b), the CSU manages the balance between positive and negative errors, while the WPES only adjusts its output when faced with negative frequency deviations. Fig. 17 (c) shows the resulting power imbalances after the resolute response of the AGC system, highlighting the contrast with their initial states and maintaining real power balance and frequency at the desired levels. Fig. 18 gracefully depicts the frequency deviations that occurred following the activation of the secondary reserves, leaving a lasting impression on the success of this remarkable endeavor.

4. Comparative analysis

This section provides a brief overview and careful evaluation of the

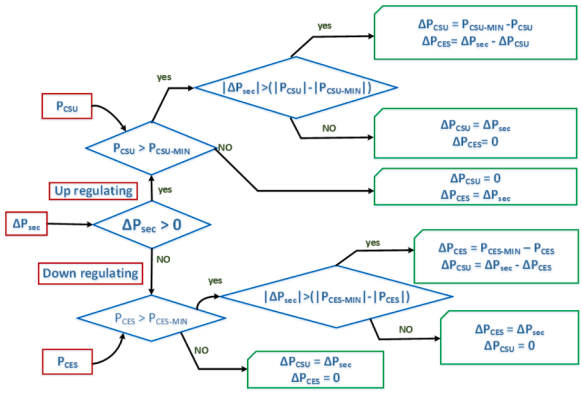

Fig. 13. Participation of CESs and CSUs into the Secondary Dispatch Process.

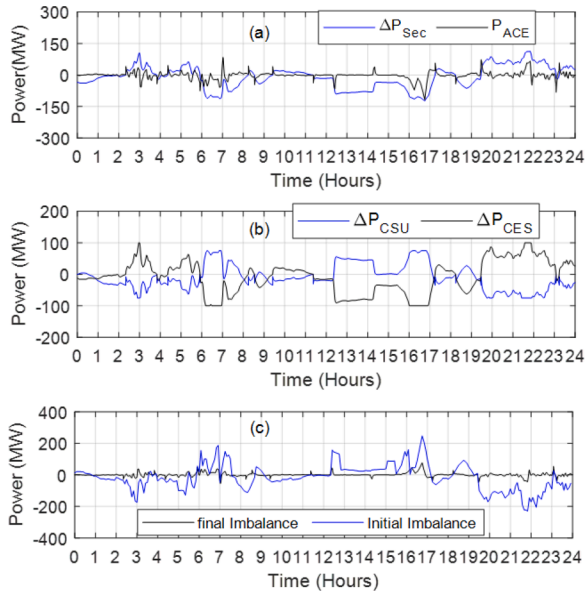

Fig. 14. (a) AGC Dispatch following area control error (b) CES and CSU individual dispatch (c) Comparison of power imbalances.

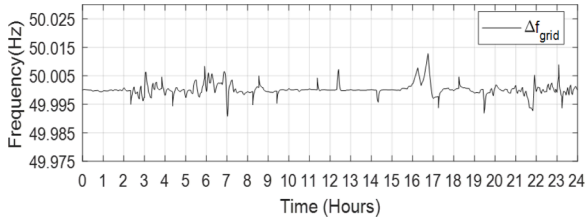

Fig. 15. Power frequency following AGC response from CES and CSUs.

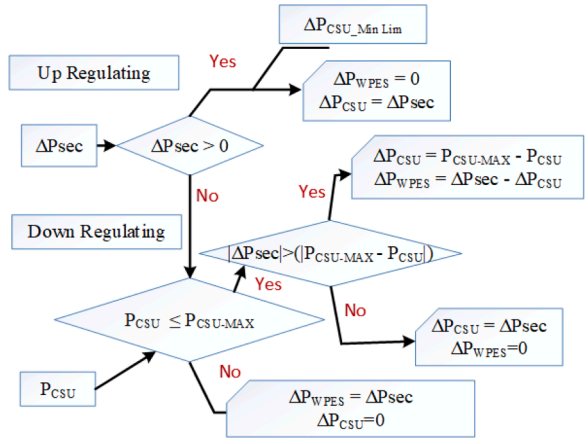

Fig. 16. Participation of WPESs and CSUs into the Secondary Dispatch Process.

outcomes achieved by the case above studies. Fig. 19 visually compares the initial power imbalance error and the subsequent results. The highest point of the initial power imbalance curve, represented by red, reaches around Ø200 MW. However, through the utilization of secondary reserves obtained in different case studies, this imbalance is successfully rectified. Initially, we focused on examining the reserves obtained only from the CESs. These reserves had a limited capacity of around 100 MW. As a result, any deviations in power that exceeded Ø100 MW remained there.

In the subsequent case study, wind power capacity alongside the CES

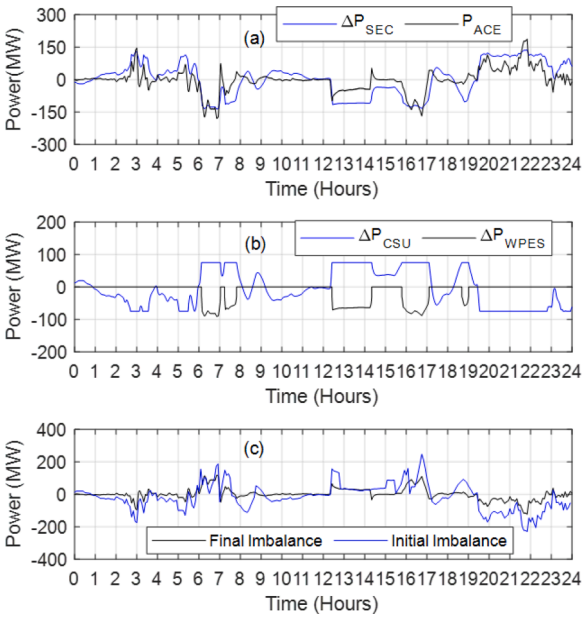

Fig. 17. (a) AGC Dispatch following area control error (b) WPESs and CSUs individual dispatch Power (c) Comparison of power imbalances.

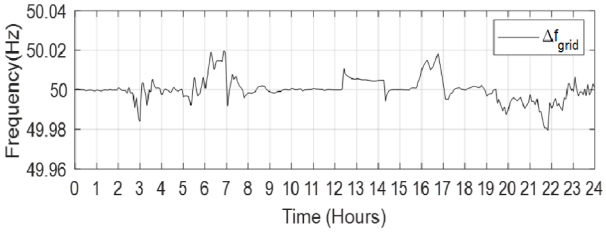

Fig. 18. Power frequency following AGC response from WPESs and CLUs.

was integrated into AGC, which led to a noticeable reduction in the disparities. The control strategy aimed to optimize costs while also dealing with the challenge of curtailing wind power during positive regulation processes. The resulting inequalities from this case study are depicted in green in Fig. 19. In Case Study 3, an optimization technique was adopted to incorporate the CSUs into the AGC dispatch strategy. With a reserve capacity of Ø75 MW, CSU was crucial in balancing these imbalances. Meanwhile, the CES acted as a reliable source of conventional power generation, operating at its lower limit to optimize the operational cost. During positive regulation, the CSU is used at its maximum capacity, while negative regulation involves carefully disengaging the CES before initiating the response of the CSUs. This case study effectively minimized power imbalances in the system network, although it led to increased CES utilization and higher operational costs. The outcomes of this study, represented by the sky-blue line, demonstrated superior error regulation compared to other case studies. In Case Study 4, the WPES replaced the reserve power provided by the CES. As a result, the system's response, depicted by the purple line in Fig. 19, became faster, leading to more efficient and economically viable operations.

Table 2 comparatively analyzes the proposed case studies, showing the quantitative differences between the initial and final power imbalances. The total area covered by positive and negative curves was calculated carefully, indicating the magnitude of imbalances. The first row shows the initial positive and negative errors that occurred due to the power imbalance between supply and demand. Subsequent rows show the respective amounts of positive and negative errors observed in various case studies. Positive and negative errors, in this case, are

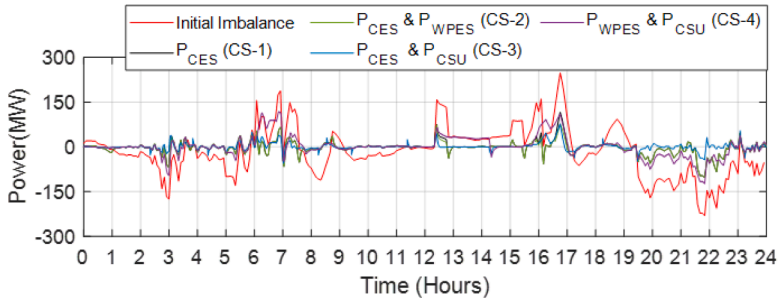

Fig. 19. Comparing initial with final power imbalances of four case studies following AGC response.

Table 2
Comparative analysis of proposed Case Studies.

Case Study	PR Area (10^6)	NR Area (10^6)	$\Delta\epsilon_{PR}$	$\Delta\epsilon_{NR}$
Initial Error $\epsilon_{initial}$	3.147	4.050	0 %	0 %
CS-01	0.4909	0.6968	84.4%	82.79%
CS-02	0.4328	0.6972	86.24%	82.79%
CS-03	0.3471	0.2368	89.0%	94.15%
CS-04	1.0126	0.8743	67.82%	78.41%

Abbreviations: CS: Case Study; NR: Negative Regulation; PR: Positive Regulation

represented by the area under the curve, carefully calculated to indicate the magnitude of imbalances. $\Delta\epsilon_{PR}$ denotes the percentage error reduced in the positive error, and $\Delta\epsilon_{NR}$ is the reduction in the magnitude of negative error as expressed in (11).

$$\Delta\epsilon_{PR/NR} = \left(\frac{\epsilon_{initial} - \epsilon_{case\ study\ (ith)}}{\epsilon_{initial}}\right) \times 100 \tag{11}$$

Table 2 shows that Case Study 3 is the most cost-effective in addressing power imbalances. In this case study, operating reserves are provided by coal energy systems and cold storage units, which significantly decrease power imbalances and offer the best solution in terms of resource allocation and maintaining the stability of the grid. The data reveals that Case Study 3 has an outstanding result of 89 percent in positive regulation error (PR) and a 94.15% decrease in negative regulation error (NR), which indicates that it is an efficient tool for maintaining power balance. Similarly, Case Study 4, which does not include conventional power plant units and only has cold storage units and wind energy systems as reserves, also shows a significant decrease in error. This case study presents a new strategy for reducing the grid reliance on conventional power plants, with relatively lower PR and NR errors than the previous case studies, though not as efficient as Case Study 3. In particular, Case Study 4 is 67 percent effective. A decrease of 82% in PR and a 78% decrease in NR. In Case Study 1, reserves were only from coal energy systems, while in Case Study 2, wind power was incorporated with the coal energy systems, and therefore, the percentage reduction in power imbalances was higher than that of Case Study 1. In Case Study 2, the addition of wind power improved the reserves strategy compared to Case Study 1, as shown in the results.

5. Conclusions

Due to stochastic wind speeds, the massive integration of wind energy into the power system requires additional reserves from traditional power sources. This leads to increased operational costs and reduced system resilience during adverse conditions. Therefore, dynamic dispatch strategies for the AGC system have been developed and implemented to overcome these challenges, integrating reserves from wind and coal-based energy systems. Further, the potential of cold storage units has been utilized to support the grid during power balancing operations. The active power support to the grid is provided via the coordinated operation of various generating units, such as cold storage units, coal-based energy systems, and wind power energy systems, and is divided into four case studies. The four case studies are comprehensively compared using graphical and quantitative analysis. The area under the curve for positive and negative regulation was calculated and compared, illustrating the extent of the reduction in area control error. The first case study integrated the operational reserves solely from coal-based energy systems (CESs) and achieved a reduction of 84.4% in positive regulation error (PR) and 82.79% in negative regulation error (NR). The second case study integrated the wind power reserves and the CES to perform the power balancing operation, resulting in slightly better reductions of 86.24% in PR error and 82.79% in NR error. Case study 3 was the most effective, with reductions of 89% in PR error and 94.15% in NR error, by utilizing the reserve capacity of CESs with the demand response of cold storage units. Case study 4 was the least effective, with reductions of 67.82% in PR error and 78.41% in NR error. However, in this case study, reserves were utilized solely from the wind energy system and the cold-based storage units, eliminating dependency on conventional power plants.

CRediT authorship contribution statement

Kaleem Ullah: Writing – original draft, Visualization, Validation, Software, Methodology, Investigation, Data curation, Conceptualization. **Zahid Ullah:** Writing – review & editing, Writing – original draft, Visualization, Validation, Software, Resources, Project administration, Methodology, Conceptualization. **Abdul Basit:** Writing – review & editing, Visualization, Software, Methodology, Data curation, Conceptualization. **Giambattista Gruosso:** Writing – review & editing, Writing – original draft, Validation, Supervision, Resources, Project administration, Investigation, Formal analysis, Conceptualization.

Declaration of competing interest

The authors declare that they have no known competing financial interests or personal relationships that could have appeared to influence the work reported in this paper.

Data availability

No data was used for the research described in the article.

References

[1] M.S. Mastoi, S. Zhuang, M. Haris, M. Hassan, A. Ali, Large-scale wind power grid integration challenges and their solution: a detailed review, Environ. Sci. Pollut. Res. 30 (47) (2023) 103424–103462.
[2] Y. Li, Y. Li, Wind generation, Cyber-Phys. Microgrids (2022) 77–97.
[3] K. Sukanya, P. Vijayakumar, Frequency control approach and load forecasting assessment for wind systems, Intell. Automat. Soft Comput. 35 (1) (2023).
[4] S. Hussain, C. Lai, U. Eicker, Flexibility: literature review on concepts, modeling, and provision method in smart grid, Sustain. Energy, Grids Netw. (2023) 101113.
[5] C. Li, C. Feng, J. Li, D. Hu, X. Zhu, Comprehensive frequency regulation control strategy of thermal power generating unit and ess considering flexible load simultaneously participating in agc, J. Energy Storage 58 (2023) 106394.

[6] M. Debouza, A. Al-Durra, Grid ancillary services from doubly fed induction generator-based wind energy conversion system: a review, IEEE Access 7 (2018) 7067–7081.
[7] S. Dhundhara, Y.P. Verma, Evaluation of ces and dfig unit in agc of realistic multisource deregulated power system, Int. Trans. Electric. Energy Syst. 27 (5) (2017) e2304.
[8] S. Kim, Analysis of deloaded wind power in hybrid ac/hvdc systems by frequency stability constrained optimal power flow, IEEE Access (2023).
[9] Y. Huo, G. Gruosso, Hardware-in-the-loop framework for validation of ancillary service in microgrids: feasibility, problems and improvement, IEEE Access 7 (2019) 58104–58112.
[10] E. Rebello, D. Watson, M. Rodgers, Ancillary services from wind turbines: automatic generation control (agc) from a single type 4 turbine, Wind Energy Sci. 5 (1) (2020) 225–236.
[11] K. Ullah, A. Basit, Z. Ullah, R. Asghar, S. Aslam, A. Yafoz, Line overload alleviations in wind energy integrated power systems using automatic generation control, Sustainability 14 (19) (2022) 11810.
[12] K. Ullah, M.A. Tunio, Z. Ullah, M. Ahsan, M.S. Salam, M.F. Umer, Optimal utilization of load frequency control in the future pakistan power system. 2023 18th International Conference on Emerging Technologies (ICET), IEEE, 2023, pp. 74–79.
[13] X. Cheng, J. Lin, F. Liu, Y. Qiu, Y. Song, J. Li, S. Wu, A coordinated frequency regulation and bidding method for wind-electrolysis joint systems participating within ancillary services markets, IEEE Trans. Sustain. Energy (2022).
[14] K. Ullah, M.A. Tunio, Z. Ullah, M.T. Ejaz, M.J. Anwar, M. Ahsan, R. Tandon, Ancillary services from wind and solar energy in modern power grids: a comprehensive review and simulation study, J. Renew. Sustain. Energy 16 (3) (2024).
[15] D. Yang, G.-G. Yan, T. Zheng, X. Zhang, L. Hua, Fast frequency response of a dfig based on variable power point tracking control, IEEE Trans. Ind. Appl. 58 (4) (2022) 5127–5135.
[16] Y. Ma, Z. Hu, Y. Song, Hour-ahead optimization strategy for shared energy storage of renewable energy power stations to provide frequency regulation service, IEEE Trans. Sustain. Energy 13 (4) (2022) 2331–2342.
[17] K. Peddakapu, M. Mohamed, P. Srinivasarao, Y. Arya, P. Leung, D. Kishore, A state-of-the-art review on modern and future developments of agc/lfc of conventional and renewable energy-based power systems, Renew. Energy Focus 43 (2022) 146–171.
[18] S. Rangi, S. Jain, Y. Arya, Utilization of energy storage devices with optimal controller for multi-area hydro-hydro power system under deregulated environment, Sustain. Energy Technol. Assess. 52 (2022) 102191.
[19] K. Peddakapu, M. Mohamed, P. Srinivasarao, Y. Arya, Assessment of energy storage and renewable energy sources-based two-area microgrid system using optimized fractional order controllers, J. Energy Storage 86 (2024) 111191.
[20] G. Sahoo, R.K. Sahu, S. Panda, N.R. Samal, Y. Arya, Modified harris hawks optimization-based fractional-order fuzzy pid controller for frequency regulation of multi-micro-grid, Arab. J. Sci. Eng. 48 (11) (2023) 14381–14405.
[21] K.E. Fahim, L.C. De Silva, F. Hussain, S.A. Shezan, H. Yassin, An evaluation of asean renewable energy path to carbon neutrality, Sustainability 15 (8) (2023) 6961.
[22] M.F. Ishraque, A. Rahman, S.A. Shezan, G. Shafiullah, A.H. Alenezi, M.D. Hossen, N.E.N. Bintu, Design optimization of a grid-tied hybrid system for a department at a university with a dispatch strategy-based assessment, Sustainability 16 (7) (2024) 2642.
[23] R. Muppidi, R.S. Nuvvula, S. Muyeen, S.A. Shezan, M.F. Ishraque, Optimization of a fuel cost and enrichment of line loadability for a transmission system by using rapid voltage stability index and grey wolf algorithm technique, Sustainability 14 (7) (2022) 4347.
[24] K. Punitha, A. Rahman, A. Radhamani, R.S. Nuvvula, S.A. Shezan, S.R. Ahammed, P.P. Kumar, M.F. Ishraque, An optimization algorithm for embedded raspberry pi pico controllers for solar tree systems, Sustainability 16 (9) (2024) 3788.
[25] M. Shaik, D.N. Gaonkar, R.S. Nuvvula, S. Muyeen, S.A. Shezan, G. Shafiullah, Nataf-kerneldensity-spline-based point estimate method for handling wind power correlation in probabilistic load flow, Expert Syst. Appl. 245 (2024) 123059.
[26] S.A. Shezan, M.F. Ishraque, G. Shafiullah, I. Kamwa, L.C. Paul, S. Muyeen, N. Ramakrishna, M.Z. Saleheen, P.P. Kumar, Optimization and control of solar-wind islanded hybrid microgrid by using heuristic and deterministic optimization algorithms and fuzzy logic controller, Energy Rep. 10 (2023) 3272–3288.
[27] M.V. Varaprasad, N. Ramakrishna, I. Kamwa, M. Venkatesan, D.M. Swamy, S. Muyeen, S.A. Shezan, M.F. Ishraque, Design and analysis of pv fed high-voltage gain dc-dc converter using pi and nn controllers, Ain Shams Eng. J. 14 (8) (2023) 102061.
[28] A. Nikoobakht, J. Aghaei, Igdt-based robust optimal utilisation of wind power generation using coordinated flexibility resources, IET Renew. Power Generat. 11 (2) (2017) 264–277.
[29] J. García-González, A. Contreras, C. Formozo, M. Vallés, E. Rivero, E. Lobato, A. Ramos, P. Frías, I. Egido, P. Sánchez, et al., Economic impact analysis of the demonstrations in task-forces tf1 and tf3-deliverable d15. 1: Wp15. economic impacts of the demonstrations, barriers towards scaling up and solutions(2014).
[30] A. Aziz, A.T. Oo, A. Stojcevski, Analysis of frequency sensitive wind plant penetration effect on load frequency control of hybrid power system, Int. J. Electric. Power Energy Syst. 99 (2018) 603–617.
[31] Z. Ullah, I. Hussain, A. Mahrouch, K. Ullah, R. Asghar, M.T. Ejaz, M.M. Aziz, S.F. M. Naqvi, A survey on enhancing grid flexibility through bidirectional interactive electric vehicle operations, Energy Rep. 11 (2024) 5149–5162.
[32] B. Shaker, K. Ullah, Z. Ullah, M. Ahsan, M. Ibrar, M.A. Javed, Enhancing grid resilience: leveraging power from flexible load in modern power systems. 2023 18th International Conference on Emerging Technologies (ICET), IEEE, 2023, pp. 246–251.
[33] G. Gruosso, Analysis of impact of electrical vehicle charging on low voltage power grid. 2016 International Conference on Electrical Systems for Aircraft, Railway, Ship Propulsion and Road Vehicles & International Transportation Electrification Conference (ESARS-ITEC), IEEE, 2016, pp. 1–6.
[34] J.D. Valladolid, D. Patino, G. Gruosso, C.A. Correa-Flórez, J. Vuelvas, F. Espinoza, A novel energy-efficiency optimization approach based on driving patterns styles and experimental tests for electric vehicles, Electronics 10 (10) (2021) 1199.
[35] Z. Ullah, K. Ullah, C. Diaz-Londono, G. Gruosso, A. Basit, Enhancing grid operation with electric vehicle integration in automatic generation control, Energies 16 (20) (2023) 7118.
[36] S. Gao, R. Dai, W. Cao, Y. Che, Combined provision of economic dispatch and frequency regulation by aggregated evs considering electricity market interaction, IEEE Trans. Transp. Electrificat. 9 (1) (2022) 1723–1735.
[37] A. Basit, T. Ahmad, A. Yar Ali, K. Ullah, G. Mufti, A.D. Hansen, Flexible modern power system: real-time power balancing through load and wind power, Energies 12 (9) (2019) 1710.

Kaleem Ullah is an accomplished electrical engineer specializing in power systems. He earned his PhD in Electrical Engineering (Power) from the University of Engineering and Technology Peshawar. During his PhD, he conducted extensive research on real-time dynamic dispatch strategies for Automatic Generation Control (AGC) mechanisms, focusing on integrating large-scale wind power into the grid while maintaining active power balance and enhancing system reliability. USAID Pakistan funded his work through an applied research grant. Dr Ullah has published several research articles on AGC modelling and designing for wind-based power systems. He secured a significant grant from the Pakistan Science Foundation for his research project on load dispatch control for the Pakistan Power System.

Zahid Ullah (Graduate Student Member) received his BS and MS in Electrical Engineering from UET Peshawar and COMSATS University Islamabad, Abbottabad Campus, Abbottabad, Pakistan, in 2014 and 2017, respectively. He is pursuing a Ph.D. in Electrical Engineering with Politecnico di Milano, Italy. He has worked as a Lecturer at UMT Lahore, Pakistan. His research interests include Smart Grid, Energy Management, Renewable Energy Systems, and ICTs for Power Systems.

Abdul Basit obtained his B.Sc. degree in electrical engineering from the University of Engineering and Technology (UET) in Peshawar, Pakistan 2006. Continuing his academic pursuits, he achieved an M.Sc. degree in electrical power engineering from Chalmers University of Technology in Sweden in 2011. Dr. Basit subsequently completed his Ph.D. in the Department of Wind Energy at the Technical University of Denmark (DTU) in 2015. He has served as an Assistant Professor at the US-Pakistan Centre for Advanced Studies in Energy (PCASE-E), UET Peshawar. Currently, he holds the position of Manager R&D at the National Power Control Center in Pakistan. His research interests encompass predictive maintenance, renewable power integration, power factor improvement, power system operation, and power system protection.

Giambattista Gruosso (Senior Member, IEEE) was born in 1973. He received the B.S. and M.S. degrees in electrical engineering and the Ph.D. degree in electrical engineering from Politecnico di Torino, Italy, in 1999 and 2003, respectively. From 2002 to 2011, he was an Assistant Professor with the Department of Electronics and Informatics, Politecnico di Milano, where he has been an Associate Professor since 2011. He is the author of more than 80 papers in journals and conferences on the topics. He does research in electrical engineering, electronic engineering, and industrial engineering. His research interests include electrical vehicles transportation electrification, electrical power systems optimization, the simulation of electrical systems, digital twins for smart mobility, factory and city, and how they can be obtained from data.